









ARFI shear-wave elastography with simulation of acute urinary tract obstruction in an *ex vivo* porcine kidney model

Jens Muttray 
 Arianeb Mehrabi 
 Mohammadreza Hafezi 
 Arash Saffari 
 Thi Thanh Tam Bui-Ta 
 Jochen Meyburg 
 Elke Wühl* 
 Jens Peter Schenk* 

PURPOSE

We aimed to evaluate if acoustic radiation force impulse (ARFI) shear-wave elastography (SWE) can detect change of parenchymal stiffness in an *ex vivo* porcine kidney model of acute urinary tract obstruction.

METHODS

A total of 20 heparinized pig kidneys were investigated at 10 intrapelvic hydrostatic pressure steps (0–90 mmHg). SWE (ARFI; Virtual Touch™ IQ, Siemens) measurements were taken at three different measuring regions and in two measuring sequences using a linear ultrasonography probe (9L4, Siemens). Median values of 10 shear-wave speed (SWS) measurements were calculated for each pressure step. Logarithmic transformed median SWS values were analyzed in a linear mixed model.

RESULTS

SWS increased significantly with increasing intrapelvic pressure. Median SWS for all kidneys in both measuring sequences and all measuring regions was 1.47 m/s (interquartile range [IQR], 0.38 m/s) at 0 mmHg, 1.94 m/s (IQR, 0.42 m/s) at 30 mmHg, 2.07 m/s (IQR, 0.43 m/s) at 60 mmHg, 2.24 m/s (IQR, 0.49 m/s) at 90 mmHg. The correlation between pelvic pressure increase and median SWS values for the central parenchyma was significantly higher compared with the peripheral parenchyma.

CONCLUSION

Acutely increased renal pelvic pressure correlates with increasing SWS values in ARFI elastography in an *ex vivo* porcine kidney model.

Urinary tract obstruction in adults is mostly acute and cannot only occur as a result of obstructing kidney stones but also as a result of rapidly growing tumors. Urinary tract obstruction is a relatively rare cause of significant acute kidney injury; however, it is associated with two-fold higher risk of chronic kidney disease (CKD) independent of other known CKD risk factors (1). In contrast to adults, obstructive uropathies in children are mostly chronic due to congenital obstructive uropathies and are the underlying renal condition in 22% of pediatric CKD patients in the registry of the North American Pediatric Renal Trials and Collaborative Studies (NAPRTCS) (2, 3). Acute obstruction, if quickly corrected, is readily reversible. Early diagnosis and treatment of obstructive uropathy might prevent or delay chronic renal damage and the risk of future renal replacement therapy.

The primary approach in imaging is ultrasonography (US) examination. However, a routine US examination will show renal morphology only; it does not discriminate between obstructive and nonobstructive dilatations of the urinary tract and does not provide information on the clinical relevance of an obstruction. For this purpose additional examinations such as renal scintigraphy are required.

A new promising method called point shear-wave elastography (SWE) with acoustic radiation force impulse (ARFI) technology, integrated into the conventional US system, allows the assessment of tissue elasticity during the US examination. An increase in parenchymal stiffness comes along with increasing shear-wave speed (SWS) values. In urinary tract ob-

From the Division of Pediatric Radiology, Clinic of Diagnostic and Interventional Radiology (J.M., T.T.B.-T., J.P.S. ✉ Jens-Peter.Schenk@med.uni-heidelberg.de), Department of Visceral and Transplantation Surgery (A.M., M.H., A.S.), Clinic I, Center for Pediatrics and Adolescent Medicine (J.M.), Division of Pediatric Nephrology, Clinic I, Center for Pediatrics and Adolescent Medicine (E.W.), University of Heidelberg School of Medicine, Heidelberg, Germany.

*Both authors contributed equally to this work.

Received 24 September 2017; revision requested 25 October 2017; last revision received 8 April 2018; accepted 17 April 2018.

DOI 10.5152/dir.2018.17353

You may cite this article as: Muttray J, Mehrabi A, Hafezi M, et al. ARFI shear-wave elastography with simulation of acute urinary tract obstruction in an *ex vivo* porcine kidney model. *Diagn Interv Radiol* 2018; 24:308-315.

struction, elevated renal pelvic pressure could be observed (4) and it is reasonable to assume that this will also influence renal tissue stiffness. Normal pelvic pressure *in vivo* in humans is close to 0 mmHg. Short episodes of higher pressure in the ureter can be caused by physiologic peristaltic waves, but the pressure in renal pelvis normally remains low. In the first minutes after acute urinary tract obstruction, reflective hyperperfusion and increased diuresis of the kidney and factors like an increase in muscular peristaltic may lead to a fast increase in pelvic pressure up to 70 mmHg (5). Within days, the renal hyperperfusion turns into a hypoperfusion and the muscular hyperperistaltic turns into hypoperistaltic with a consecutively normal to low intrarenal pelvic pressure.

A similar constellation of obstruction, tissue stiffness, and increased SWS was already shown for obstructive diseases of the biliary system (6) and of the salivary glands (7). While in adult patients with acute hydronephrosis caused by ureteral stones an increase of SWS values was observed (8), situation in pediatric patients with acute or chronic urinary tract obstruction is still unclear. Preliminary data in pediatric patients suggest that in patients with vesicoureteral reflux SWS was increased (9); however, in patients with ureteropelvic junction obstruction Habibi et al. (10) found lower SWS values.

In order to simulate acute urinary tract obstruction, we developed an *ex vivo* porcine kidney model for SWE examination to evaluate the effect of stepwise renal pelvic pressure increase and decrease on tissue stiffness and SWS.

Methods

Experimental approach

All institutional and national guidelines for the care and use of laboratory animals were

Main points

- Acutely increased renal pelvic pressure correlates with increasing shear-wave speed (SWS) values in acoustic radiation force impulse (ARFI) elastography in an *ex vivo* porcine kidney model.
- Measuring in the parenchyma next to the renal pelvis comes along with the highest correlation between intrarenal pelvic pressure and SWS.
- The ARFI elastography might be helpful to identify increased intrarenal pelvic pressure in patients with acute urinary tract obstruction.



Figure 1. Kidney specimen preparation with a purse-string suture and a cable strap.

followed, including the NIH guidelines for the use of laboratory animals, in this study.

A total of 20 pig kidneys were examined by SWE in an *ex vivo* approach. Fresh cadaver kidneys were collected from euthanized pigs. After explantation, each kidney specimen was flushed via the renal arteries with heparin solution (1000 IU Heparin/20 mL sodium chloride 0.9%) (B. Braun Medical). The renal specimens were cooled in physiologic saline solution at approximately 5°C for transportation to US examination unit within 30 min. In the experimental set-up the kidneys were put into a measuring tank filled with 7.5 cm new saline solution, measurements themselves were performed at a temperature of 20°C equivalent to the ambient temperature. The cut off end of a Heidelberg extension tube with an inner diameter of 3.0 mm and an outer diameter of 4.1 mm (Becton, Dickinson and Company) was prepared into the ureteral pelvic junction and fixed with a purse-string suture. In addition, the open end of the ureter was sealed by a cable strap as shown in Fig. 1 (11). A three-way stopcock (Becton, Dickinson and Company) connected the opposite end of the Heidelberg extension tube with an infusion set and the measuring probe of the pressure monitoring system (Philips IntelliVue MP5, Philips). Pelvic pressure was adjusted by raising and lowering the infusion bag containing physiologic saline solution. Thereby, the pelvic pressure was kept constant at each pressure level. SWS measurements were performed at 10 pressure

intervals of 10 mmHg each ranging from 0 to 90 mmHg. As soon as the pressure monitoring system showed constant pelvic pressure for at least 10 s, SWE measurements were started.

Elastography

B-mode US and SWE (Virtual Touch™ IQ, Siemens) were performed using the US system Acuson HELX™ Evolution S3000 (Siemens) with a linear US probe (9L4, Siemens). To exclude external pressure to the renal surface the probe was clamped on a laboratory stand. Thus, a minimal deviation of the measuring position could be achieved for each series of measurements (12). The US probe and the renal surface were positioned right-angled to each other in the saline solution. The distance between the probe and the renal surface was set at 1 cm at a pelvic pressure level of 0 mmHg, in order to achieve a more constant depth for the ARFI measurements. As the renal surface is not completely plane but curved, the positioning of the US probe was subject to slight inaccuracies.

For each pressure level a conventional B-mode image (Figs. 2a, 3a) and a quality map (Figs. 2b, 3b) were saved. Regions of interest (ROIs) were only placed in regions of maximum quality (color-coded in green in the quality map). Ten SWS measurements were performed at each pressure level by setting 10 ROIs next to each other as shown in Figs. 2c, 3c. In order to characterize reversibility of the effect of pelvic pressure, SWS measurements were per-

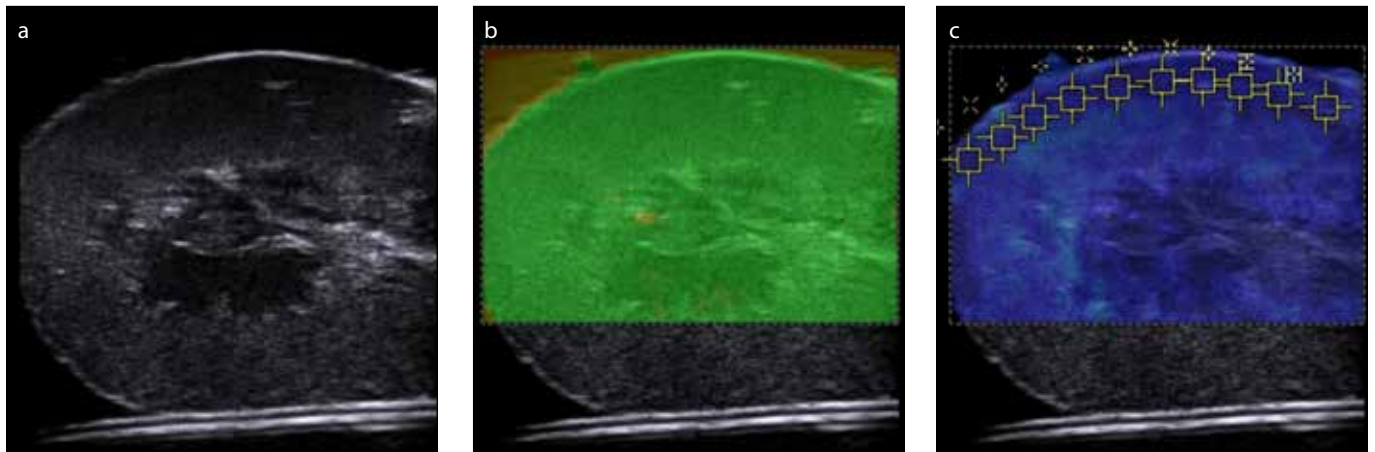


Figure 2. a–c. Conventional B-mode US (a), quality map (b) and ARFI-Virtual Touch IQ elastography image with 10 ROIs in the peripheral parenchyma region (c) at a pressure level of 0 mmHg (kidney 19).

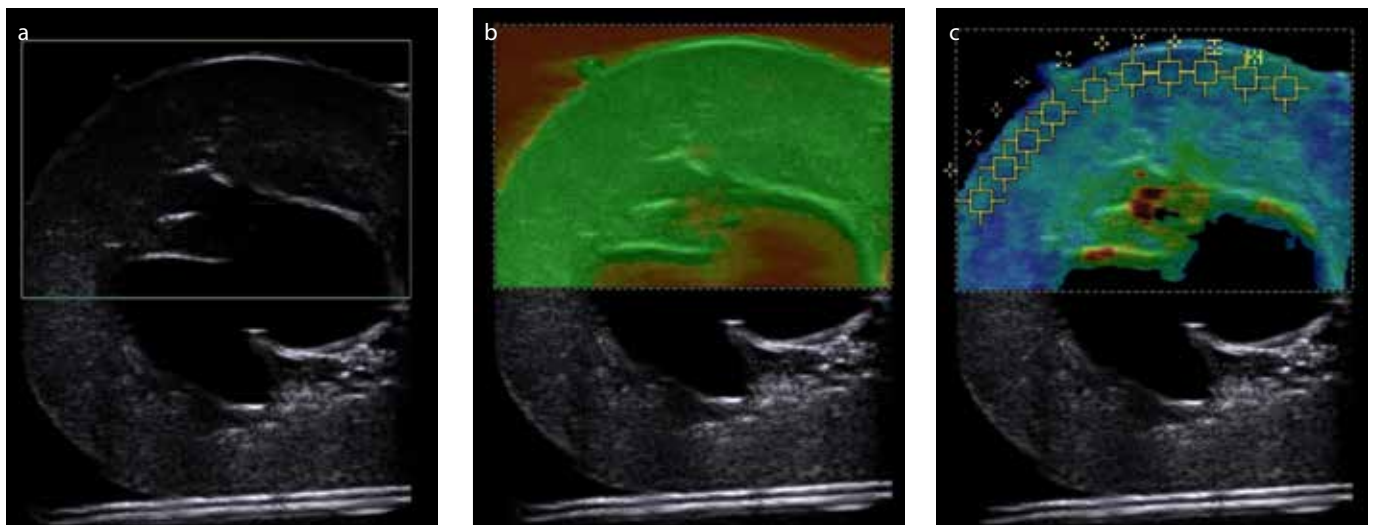


Figure 3. a–c. Conventional B-mode US (a), quality map (b) and ARFI-Virtual Touch IQ elastography image with 10 ROIs in the peripheral parenchyma region (c) at a pressure level of 60 mmHg (kidney 19).

formed in two measuring sequences for every kidney specimen. In the first test series, called increasing sequence, the pressure was increased from 0 to 90 mmHg in steps of 10 mmHg. The following test series, called decreasing sequence, took place right after the first one for every kidney. In the decreasing sequence, the pressure was decreased 10 mmHg step by step from 90 to 0 mmHg.

The size of the rectangular ROI was 2×2 mm thus a selection of different measurement regions in the renal parenchyma was possible. Three measuring regions were defined for every measurement series to identify the highest physiologic effect on SWS according to the distance to the renal pelvis and capsule: the peripheral parenchyma region (1 cm maximum distance to the renal capsule), the intermediate parenchyma re-

gion (at least 1 cm distance to the perirenal capsule and renal pelvis) and the central parenchyma region (1 cm maximum distance to the renal pelvis) (Fig. 4).

Statistical analysis

All statistical analyses were performed using the statistical package SAS for Windows Version 9.3 (SAS Institute Inc.). The median of 10 values in a measurement series was defined as dependent variable of a defined pelvic pressure stage because of relative robustness in case of outliers. Exploratory analysis was performed using spaghetti plots as well as linear regression plots of all kidneys. Linear regression plots were also created for every region and direction (increasing versus decreasing sequence) of measurement, in order to obtain better knowledge of the dataset for the following modeling. In order to stabilize the

variance, in a further step median SWS were log transformed. A mixed model with fixed and random effects was created (13). Random effects were defined for the individual kidneys as well as for the variability of the individual kidneys within a measuring region. As fixed effects, pressure, measuring region and direction of the measuring sequence were included. An unstructured covariance structure was assumed. Parameters of the model were obtained using the restricted maximum likelihood method. Influence statistics were calculated in order to gain further knowledge about influencing factors. The significance levels were set at 5% (14).

Results

Median SWS in 20 pig kidneys, at 10 pressure levels, measured in an ascending and

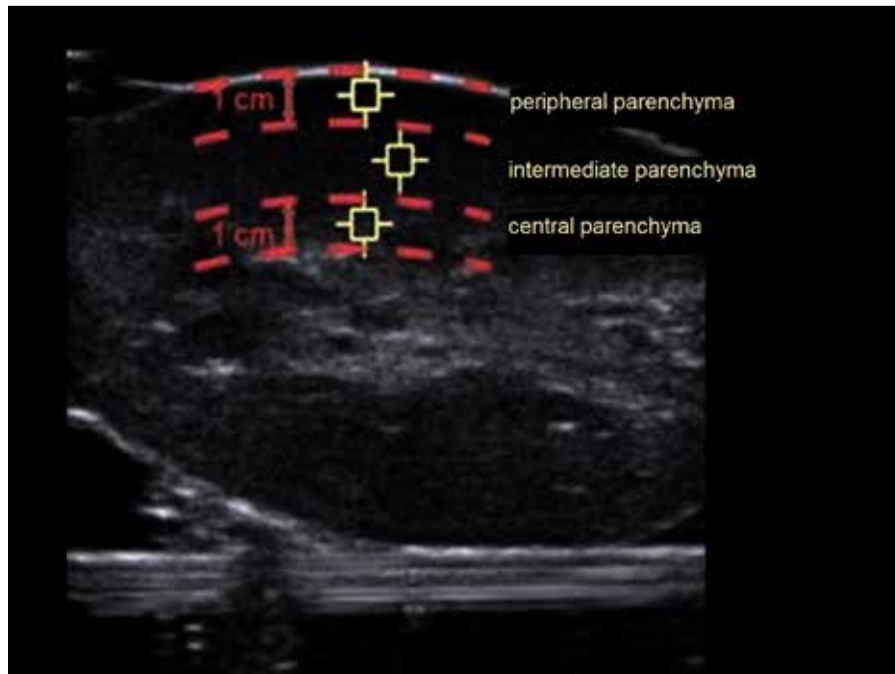


Figure 4. Edited B-mode US demonstrating the three measuring regions, defined by their distances to the peri-renal capsule and the renal pelvis.

Table 1. Median and IQR values of all SWS measurements*

Intrarenal pelvic pressure (mmHg)	SWS (m/s) Median (IQR)
0	1.47 (0.38)
10	1.68 (0.37)
20	1.83 (0.39)
30	1.94 (0.42)
40	1.98 (0.43)
50	2.04 (0.46)
60	2.07 (0.43)
70	2.09 (0.51)
80	2.15 (0.51)
90	2.24 (0.49)

Data are presented for all 20 kidneys in both measuring sequences and for all measuring regions (n=120). IQR, interquartile range; SWS, shear-wave speed.

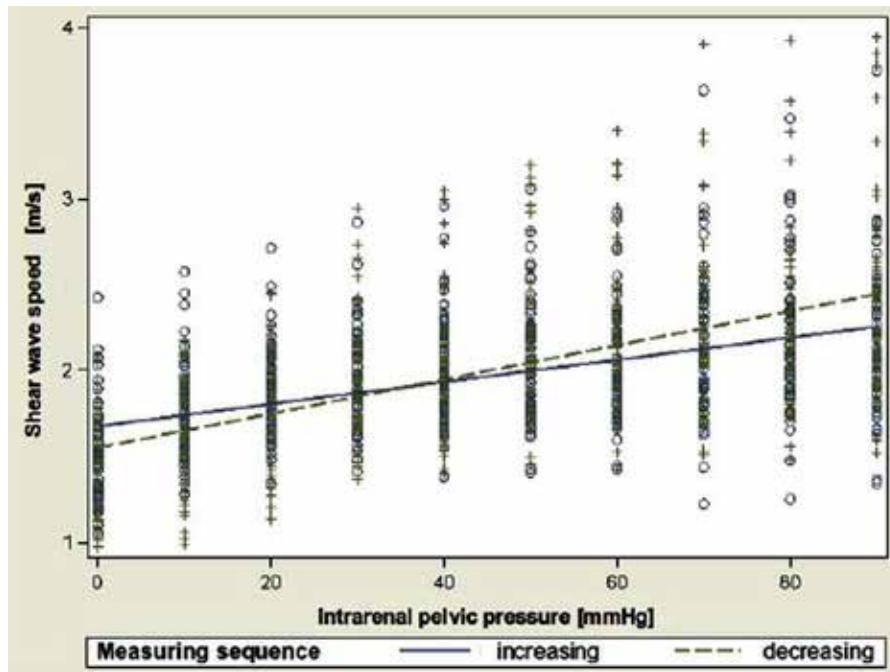


Figure 5. Regression lines for the direction of the measuring sequences.

descending sequence each, as well as in three different regions, resulted in a total of 1200 SWS values (range, 0.97–3.95 m/s) without any missing values.

Regarding the effect of intrapelvic pressure on SWS values in all measurements, the median of SWS by defined pressure levels revealed a SWS of 1.47 m/s (inter-

quartile range [IQR], 0.38 m/s) at a pressure level of 0 mmHg, 1.94 m/s (IQR, 0.42 m/s) at 30 mmHg, 2.07 m/s (IQR, 0.43 m/s) at 60 mmHg and 2.24 m/s (IQR, 0.49) at 90 mmHg as shown in Table 1.

A general increase of median SWS values for increasing pelvic pressure values could be observed for all 20 kidneys. Neverthe-

less, there were kidneys showing flatter or steeper gradients of SWS rise.

Linear regression plots are shown in Fig. 5 for increasing and decreasing sequences. The median SWS values for all kidneys in lower pressure levels were lower in the increasing measuring sequence than in the decreasing measuring sequence. Fig. 6 demonstrates the results of three different measuring regions. The SWS values were similar in all three measuring regions at a pelvic pressure of 0 mmHg with marginally higher values for the intermediate parenchyma region. However, the SWS showed a steeper increase in the central parenchyma region than in the intermediate parenchyma region than in the peripheral parenchyma region. The standard deviation for all SWS medians for all pressures and both measuring sequences was 0.3831 m/s for the central parenchyma region, 0.3255 m/s for the intermediate parenchyma region and 0.1676 m/s for the peripheral parenchyma region.

The SWS change was higher for low pressure than for high pressure (Table 2). Between 0 and 30 mmHg there was an increase in median SWS of 0.47 m/s, between 30 and 60 mmHg of 0.13 m/s and between 60 and 90 mmHg of 0.17 m/s, suggesting a logarithmic correlation rather than a linear one.

By stabilizing the variance, a logarithmic correlation could be confirmed. The esti-

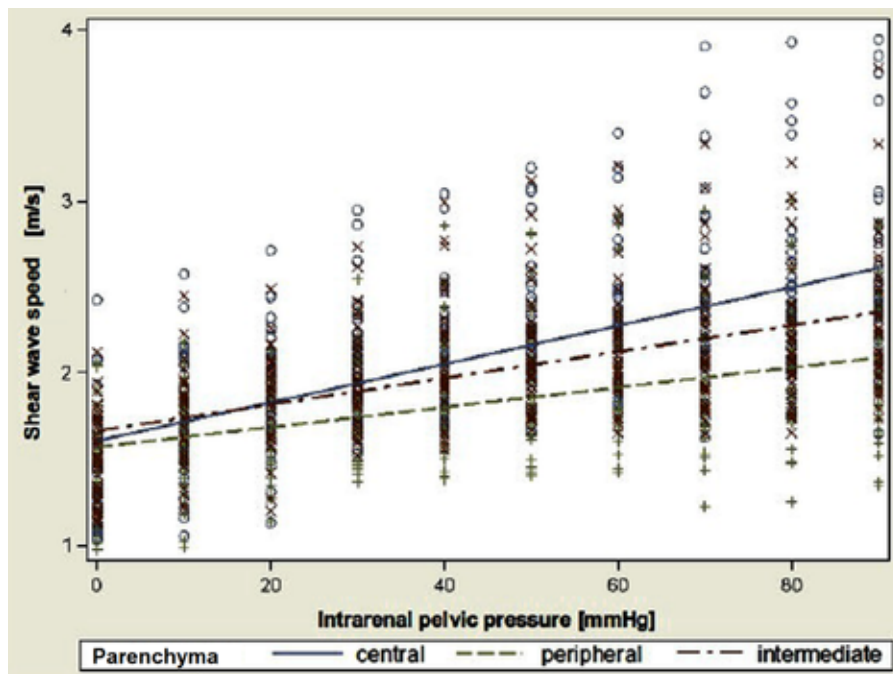


Figure 6. Regression lines for the measuring regions.

Table 2. Median SWS differences	
Intrarenal pelvic pressure differences (mmHg)	SWS differences (m/s)
10–00	0.22
20–10	0.15
30–20	0.10
40–30	0.04
50–40	0.07
60–50	0.02
70–60	0.03
80–70	0.05
90–80	0.09

Data are presented for pressure steps of 10 mmHg for all 20 kidneys in both measuring sequences and all measuring regions (n=120). SWS, shear-wave speed.

ated total variance of the linear mixed model for the logarithmic median SWS was 0.03. The estimated shared explained variation for the variable kidney (1 of 20) was 41.4%. For the variable region within a kidney it was 8.7%.

Pelvic pressure was confirmed to have a significant effect in the mixed model ($P < 0.001$). The effect remained significant after adjusting possible confounding factors

(direction, region, interactions). The estimated intercept for the log-transformed median SWS was 0.4539 ($P < 0.001$) units. The slope parameter for the effect pressure was 0.004985 ($P < 0.001$). In other words, if the pressure was increased by 10 mmHg, the logarithmic median SWS increased by 0.05 units.

There was a significant effect for the direction of the measuring sequence ($P < 0.001$) as well. The intercept of the log-transformed median SWS for the decreasing series was significantly higher than in the increasing measuring sequence (+0.09573 units, $P < 0.001$). In other words, the effect of increasing pelvic pressure on median SWS values was not fully reversible. For pressures above 30 to 40 mmHg, the log-transformed median SWS values for the increasing sequence were higher than the ones for the decreasing sequence. The estimated slope parameter was by 0.00205 units lower in the decreasing measuring sequence ($P < 0.001$). If the pressure in the increasing sequence is increased by 10 mmHg, the log-transformed SWS would increase 0.05 units, while it would only decrease 0.03 units if the pressure is decreased by 10 mmHg in the decreasing sequence.

Furthermore, a significant effect of the measuring region on SWS could be shown ($P = 0.027$). The intercept of the log-transformed median SWS values was not sig-

nificantly different for the three regions: central parenchyma region compared with intermediate parenchyma region (0.02639 units lower, $P = 0.35$), peripheral parenchyma region compared with intermediate parenchyma region (0.05112 units lower, $P = 0.075$). The slope parameter for the central parenchyma region was 0.001750 units higher than the one for the intermediate parenchyma region ($P < 0.001$). Furthermore, the slope parameter for the peripheral parenchyma region was 0.00104 units lower in comparison to the intermediate parenchyma region ($P = 0.015$). If the pressure was increased by 10 mmHg the log-transformed SWS increased by 0.07 units in the central parenchyma, by 0.05 units in the intermediate parenchyma and by 0.04 in the peripheral parenchyma region.

The estimated range for the distance between the US probe and the ROI of the ARFI measurement was 1.0–4.5 cm for a pelvic pressure of 0 mmHg and 0.9–4.5 cm for a pelvic pressure of 90 mmHg. Differences between the different kidneys including inaccuracies of the depth of ARFI measurements did not have a major influence on the parameters of the mixed model as shown by the influence statistics calculated for the mixed model.

Discussion

A relevant and significant increase of SWS values for Virtual Touch™ IQ technique with increasing pelvic pressures could be shown in the *ex vivo* porcine kidney model. The primary assumption of this study could be confirmed. A repeated measurement with 10 ROIs and calculation of the median value was proven to be practical and effective in this *ex vivo* situation. An effect of pressure on renal kidney tissue elasticity could already be shown for external pressure caused by the US transducer itself by Syversveen et al. (15). They applied compressive weights from 22 to 2990 g on patients with transplanted kidneys and measured a significant increase of median SWS of about 2.3 m/s. Gennisson et al. (16) investigated tissue elasticity in an *in vivo* pig kidney model using the supersonic shear-wave technology which is based on similar physical principles as ARFI elastography. They could show higher supersonic shear-wave values in kPa for increased pelvic pressures up to 40 mmHg in five porcine kidneys. However, in contrast to our results they assumed a linear correlation instead of a logarithmic

correlation between pelvic pressure and tissue stiffness for statistical testing. As far as we know, there is no prior study using SWE (Virtual Touch™ IQ) in a pig kidney model of increased pelvic pressure.

The effect of changing pressure on SWS provoked by different hydrostatic pressure levels in the renal pelvis in our model could not only be shown for increasing but also for decreasing pelvic pressures. However, the effect of increasing pressure on kidney tissue stiffness was not fully reversible. Thus, changes in kidney tissue integrity by the high hydrostatic pressure to the renal pelvis and tissue have to be discussed for this *ex vivo* model.

Jian Wang et al. (17) could show that a step by step increase in pelvic pressure up to 50 mmHg in porcine kidneys (steps of 10 mmHg, each pressure step maintained for 10 minutes) caused renal tubule and renal capsule dilatation and renal glomerulus compression even in healthy control kidneys (17). It can be assumed that kidney tissue damage will even be worse if the elevated pelvic pressure persists for hours or days, leading to chronic kidney damage and CKD in the worst case scenario. Against the background of the pathophysiology of urinary tract obstruction it becomes clear that measurements in this model of urinary tract obstruction were taken at relevant pressure levels including pelvic pressures from 0 to 90 mmHg. In contrast to this, Gennisson et al. (16) only measured tissue elasticity at pelvic pressures up to 40 mmHg in the *in vivo* porcine model.

This *ex vivo* model is most likely suitable to depict the clinical situation of an acute urinary tract obstruction. The most common pathology causing acute urinary tract obstruction in adults is nephrolithiasis and the lifetime risk of passing a kidney stone is about 8%–10% (18, 19).

A general recommendation for the measuring region cannot be derived from our study results. For low pressures, no significant differences in SWSs were detected for different measuring regions in our study. However, Gennisson et al. (16) found higher elasticity modulus in the inner parenchyma compared with the outer parenchyma and the medulla. They suggested that medullar anisotropy in combination with the angle between shear waves and anatomic structures might be the reason for this finding.

In our study for higher pressures, measuring in the central parenchymal region

showed the strongest correlation between intrarenal pelvic pressure and SWS. It can be assumed that the increased intrarenal pelvic pressure caused a pressure gradient across the kidney tissue with decreasing pressure, and respectively, tissue stiffness in the peripheral region. For diseases causing elevated intrarenal pelvic pressures of up to 70 mmHg, e.g., acute urinary obstruction (5), measuring in the central parenchyma region seems to be preferable.

For the assessment of ARFI-SWS values in human urinary tract obstruction, the availability of normal SWS values is essential. Graeter et al. (20) investigated ARFI values for healthy human kidneys with ARFI Virtual Touch Tissue Quantification (VTQ, Siemens). Mean SWS values for a cohort of 99 healthy adult volunteers were 2.7 ± 0.8 m/s at the midpole of the right kidney and 2.9 ± 0.9 m/s at the midpole of the left kidney (20). Compared with the SWS values described in the chapter results (Table 1) for pelvic pressures between 0 and 10 mmHg, these values are clearly higher than our *ex vivo* values. Chau Ngan et al. (8) investigated renal tissue stiffness with ARFI-SWE (VTQ, Siemens). Mean SWS values were 2.73 ± 0.4 m/s for patients with kidney stones, 1.66 ± 0.16 m/s for patients with ureteropelvic junction obstruction and 1.60 ± 0.2 m/s for the healthy control group.

Our *ex vivo* model represents also the pediatric pressure situation with pelvic pressures of <15 cm H₂O (equivalent to <11 mmHg) in healthy and >22 cm H₂O (>15 mmHg) in children with acute urinary tract obstruction (21). We could demonstrate an increase in SWS of 0.22 m/s by an increase of renal pelvic pressure from 0 to 10 mmHg and 0.15 m/s from 10 to 20 mmHg.

Children with hydronephrosis including cases with ureteropelvic junction obstruction were examined with VTQ/Siemens by Sohn et al. (22). Median SWS values in kidneys with high-grade hydronephrosis were higher than those in normal kidneys. In their cohort, patients with ureteropelvic junction obstruction had similar SWS compared with children with hydronephrotic kidneys of other causes. A recent study by Habibi et al. (10) came to contradictory results: higher SWS values were found in control kidneys compared with kidneys affected by ureteropelvic junction obstruction. Dillmann et al. (23) tried to discriminate obstructive hydronephrosis from nonobstructive hydronephrosis. A significant difference in SWS could not be demonstrated between these two groups.

In patients with vesicoureteral reflux, results of VTQ elastography are inconclusive. On one hand, it was reported by Bruno et al. (9) that kidneys affected by vesicoureteral reflux are stiffer than normal kidneys. On the other hand, decreasing SWS values were found by Göya et al. (24) for kidneys with increasing degree of vesicoureteral reflux (24). Different effects of acute and chronic processes influencing SWS should be considered. Especially the grade of renal fibrosis might be associated with higher SWS values (25, 26). These clinical results may indicate that hydronephrosis in children cannot be compared to hydronephrosis in acute urinary tract obstruction in adults caused by kidney stones with different effects on organ stiffness. Further research is required to improve the understanding of the role of SWE in the evaluation of patients with congenital hydronephrosis (27).

Furthermore, the evaluation of renal SWS values in children with VTQ or VTIQ techniques is difficult as only very few ARFI SWS standard values have been published so far. Lee et al. (28) determined mean SWS values of 2.19 m/s for the right kidney and 2.33 m/s for the left kidney in a cohort of 202 normal pediatric patients. This level of SWE is similar to the SWS values measured in our porcine renal specimen with high pelvic pressure in our study with VTIQ technique. In a recent paper of Grass et al. (29), SWS in healthy children measured with VTIQ was 1.96 ± 0.27 m/s, equivalent to values measured at 30 mmHg in our model.

The position of the sample volume for SWS measurement is of major interest in SWE. When VTQ technique in clinical situation often is not able to discriminate between different positions to the renal pelvis, VTIQ technique has much smaller ROI with a possibility to select a different position. Bruno et al. (30) describe medullar anisotropy and resulting higher variability in SWS values as a basis to recommend ARFI measurements in the outer renal parenchyma excluding medullary pyramids. It has to be stated that measurements in the inner parenchyma region in this study could not exclude medullary pyramids. A higher variability of SWS values in the central parenchyma region compared with the peripheral parenchyma region was reflected by a higher standard deviation of SWS medians in this study as well (± 0.3831 m/s for the central parenchyma region compared with ± 0.1676 m/s for the peripheral parenchyma region).

The results of our study may indeed be of concrete clinical use for patients with acute obstruction to demonstrate a high pressure level. SWS measurements might help in the monitoring of the pelvic pressure situation after interventions such as placing a double J stent. SWS values before and after the intervention might provide knowledge about the success of pressure relief. This clinical application seems to be particularly promising as the SWS rise in the *ex vivo* pig kidney model was mostly reversible in the decreasing measuring sequence.

In the clinical context we see a potential of SWE to discriminate between acute and chronic hydronephrosis. It has to be mentioned that it might be difficult to achieve constant measurements in real clinical patients. Variability might be caused by non-compliance of the patient as well as by a deeper anatomical position of the kidney compared with the *ex vivo* model.

Limitations of this *ex vivo* renal specimen model have to be considered. First, anatomic differences between human and porcine kidneys exist; two types of papillae (single and compound) can be found in different frequency in human and porcine kidneys. Fused compound papillae are more frequent in pig kidneys with different morphology of orifices (31, 32). Second, pressure generated by the investigator is a confounding factor mainly in *in vivo* situations (33). It could be completely excluded in this model. But this is not a situation we expect in the clinical routine. Third, SWE in our study was done by one examiner familiar with the porcine model. But interoperator reproducibility was described as another possible confounding factor in ARFI SWE (34) in a clinical study. Finally, the period of time between explantation and the beginning of measurements as well as temperature fluctuations may have resulted in minor kidney tissue alterations and changes in tissue stiffness. This is an unpreventable difference of the *ex vivo* compared with an *in vivo* model. The influence of perfusion of a kidney is another major effect on SWE which is excluded in our model, but we could demonstrate the principal change of SWS (VTIQ technique) in kidney parenchyma, which is of importance for further research of *in vivo* situations. There were slight changes in the depth of the ARFI measurements. A plastic deformation of the kidneys due to changing intrapelvic pressure and concomitant fluctuations of the depth of

measurements could not be prevented by fixation of the kidneys. The measuring conditions were not completely constant for all kidneys. This represents a possible limitation of the model. However, *in vivo* studies with humans have shown that the depth of measurement has no significant impact on the ARFI SWS (29, 35).

In conclusion, acutely increased pelvic pressure correlates with increasing SWS values in SWE in an *ex vivo* porcine kidney model. The increase of tissue stiffness is almost completely reversible with descending pelvic pressures. While our findings are promising with respect to the clinical evaluation in patients with acute urinary tract obstruction, use of SWE in patients with chronic obstruction warrants further research.

Conflict of interest disclosure

The authors declared no conflicts of interest.

References

- Keddis MT, Rule AD. Nephrolithiasis and loss of kidney function. *Curr Opin Nephrol Hypertens* 2013; 22:390–396. [CrossRef]
- Harmon W, Stablein D, Talley L, et al. North American Pediatric Renal Transplant Cooperative Study. 2005 Annual Report. 2005; 13:1–4.
- Warady BA, Chadha V. Chronic kidney disease in children: the global perspective. *Pediatr Nephrol* 2007; 22:1999–2009. [CrossRef]
- Tepeler A, Akman T, Silay MS, et al. Comparison of intrarenal pelvic pressure during micro-percutaneous nephrolithotomy and conventional percutaneous nephrolithotomy. *Urolithiasis* 2014; 42:275–279. [CrossRef]
- Cochlin D, Dubbins P, Alexander A. *Urogenital ultrasound: a text atlas*. UK: CRC Press, 1994; 48–49.
- Attia D, Pischke S, Negm A, et al. Changes in liver stiffness using acoustic radiation force impulse imaging in patients with obstructive cholestasis and cholangitis. *Dig Liver Dis* 2014; 46:625–631. [CrossRef]
- Zengel P, Schrötzmair F, Schwarz F, et al. Elastography: a new diagnostic tool for evaluation of obstructive diseases of the salivary glands; primary results. *Clin Hemorheol Microcirc* 2012; 50:91–99.
- Chau Ngan T, Hung Thien N, Hai Thanh P. Acoustic radiation force impulse assessment of hydronephrosis in adults in an out patient clinic. *Ultrasound Med Biol* 2015; 41:142. [CrossRef]
- Bruno C, Caliarì G, Zaffanello M, et al. Acoustic radiation force impulse (ARFI) in the evaluation of the renal parenchymal stiffness in paediatric patients with vesicoureteral reflux: preliminary results. *Eur Radiol* 2013; 23:3477–3484. [CrossRef]
- Habibi H, Cicek R, Kandemirli S, et al. Acoustic radiation force impulse (ARFI) elastography in the evaluation of renal parenchymal stiffness in patients with ureteropelvic junction obstruction. *J Med Ultrason* 2017; 44:167–172. [CrossRef]

- Schenk JP, Friebe B, Ley S, et al. Visualization of intrarenal vessels by 3.0-T MR angiography in comparison with digital subtraction angiography using renal specimens. *Pediatr Radiol* 2006; 36:1075. [CrossRef]
- Cygan S, Januszewicz M. Acoustic radiation force impulse imaging of kidneys – a phantom study. *J Ultrason* 2016; 16:329–338. [CrossRef]
- West BT, Welch KB, Galecki AT. *Linear mixed models: A practical guide using statistical software*. Boca Raton: Taylor & Francis Group, 2007; 11–13.
- Bender R, Lange ST, Ziegler A. *Multiples Testen*. *Dtsch Med Wochenschr* 2002; 127:T4–T7.
- Syversveen T, Midtvedt K, Berstad AE, Brabrand K, Strøm EH, Abildgaard A. Tissue elasticity estimated by acoustic radiation force impulse quantification depends on the applied transducer force: an experimental study in kidney transplant patients. *Eur Radiol* 2012; 22:2130–2137. [CrossRef]
- Gennisson JL, Grenier N, Combe C, Tanter M. Supersonic shear wave elastography of *in vivo* pig kidney: influence of blood pressure, urinary pressure and tissue anisotropy. *Ultrasound Med Biol* 2012; 38:1559–1567. [CrossRef]
- Wang J, Zhou DQ, He M, et al. Effects of renal pelvic high-pressure perfusion on nephrons in a porcine pyonephrosis model. *Exp Ther Med* 2013; 5:1389–1392. [CrossRef]
- Parmar MS. Kidney stones. *BMJ* 2004; 328:1420–1424. [CrossRef]
- Asplin JR, Favus MJ, Coe FL. Nephrolithiasis. In: Brenner BM, editor. *Brenner and Rector's the kidney*. 5th ed. Philadelphia: Saunders, 1996; 1893–1935.
- Graeter T, Boretzki S, Nuraldeen R, et al. A pilot study to generate standard values of acoustic radiation force impulse – virtual touch tissue quantification of the kidneys in healthy subjects. *Ultraschall in Med* 2013; 34:PS4_03.
- Towbin R, Baskin K. *Pediatric Interventional Radiology*. Cambridge: Cambridge University Press, 2015; 320–321. [CrossRef]
- Sohn B, Kim MJ, Han SW, Im YJ, Lee MJ. Shear wave velocity measurements using acoustic radiation force impulse in young children with normal kidneys versus hydronephrotic kidneys. *Ultrasonography* 2014; 33:116–121. [CrossRef]
- Dillman JR, Smith EA, Davenport MS, et al. Can shear-wave elastography be used to discriminate obstructive hydronephrosis from nonobstructive hydronephrosis in children? *Radiology* 2015; 277:259–267. [CrossRef]
- Göya C, Hamidi C, Ece A et al. Acoustic radiation force impulse (ARFI) elastography for detection of renal damage in children. *Pediatr Radiol* 2015; 45:55–61. [CrossRef]
- Cui G, Yang Z, Zhang W et al. Evaluation of acoustic radiation force impulse imaging for the clinicopathological typing of renal fibrosis. *Exp Ther Med* 2014; 7:233–235. [CrossRef]
- Stock KF, Klein BS, Vo Cong MT, et al. ARFI-based tissue elasticity quantification in comparison to histology for the diagnosis of renal transplant fibrosis. *Selected Papers from the 28th Congress on Clinical Hemorheology and Microcirculation of the German Society*, Munich, Germany, 20–21 November 2009.

27. Wang L. Applications of acoustic radiation force impulse quantification in chronic kidney disease: a review. *Ultrasonography* 2016; 35:302–308. [\[CrossRef\]](#)
28. Lee MJ, Kim MJ, Han KH, Yoon CS. Age-related changes in liver, kidney, and spleen stiffness in healthy children measured with acoustic radiation force impulse imaging. *Eur J Radiol* 2013; 82:e290–e294. [\[CrossRef\]](#)
29. Grass L, Szekeley N, Alrajab A, Bui-Ta T, Hoffmann G, Wühl E, Schenk J-P. Point shear wave elastography (pSWE) using Acoustic Radiation Force Impulse (ARFI) imaging: a feasibility study and norm values for renal parenchymal stiffness in healthy children and adolescents. *Med Ultrason* 2017; 19:366-373. [\[CrossRef\]](#)
30. Bruno C, Minniti S, Bucci A, Pozzi Mucelli R. ARFI: from basic principles to clinical applications in diffuse chronic disease—a review. *Insights Imaging* 2016; 7:735–746. [\[CrossRef\]](#)
31. Thomsen HS, Larsen S, Talner LB. Papillary morphology in adult human kidneys and in baby and adult pig kidneys. *Eur Urol* 1983; 9:170–180. [\[CrossRef\]](#)
32. Thomsen HS, Dorph S, Larsen S, Talner LB. Intrarenal backflow and renal perfusion during increased intrapelvic pressure in excised porcine kidneys. *Acta Radiol Diagn* 1983; 24:327–336. [\[CrossRef\]](#)
33. Syversveen T, Midtvedt K, Berstad AE, Brabrand K, Strøm EH, Abildgaard A. Tissue elasticity estimated by acoustic radiation force impulse quantification depends on the applied transducer force: an experimental study in kidney transplant patients. *Eur Radiol* 2012; 22:2130–2137. [\[CrossRef\]](#)
34. Bob F, Bota S, Sporea I, Sirli R, Petrica L, Schiller A.. Kidney shear wave speed values in subjects with and without renal pathology and inter-operator reproducibility of acoustic radiation force impulse elastography (ARFI) - preliminary results. *PLoS ONE* 2014; 9:e113761. [\[CrossRef\]](#)
35. Sagir A, Ney D, Oh J, et al. Evaluation of acoustic radiation force impulse imaging (ARFI) for the determination of liver stiffness using transient elastography as a reference in children. *Ultrasound Int Open* 2015; 1:E2–E7. [\[CrossRef\]](#)